PHYSICAL REVIEW D **85,** 115025 (2012)

Saving the fourth-generation Higgs boson with radion mixing

Mariana Frank,[1,*] Beste Korutlu,[1,†] and Manuel Toharia[1,‡]

[1]*Department of Physics, Concordia University, 7141 Sherbrooke St. West, Montreal, Quebec, Canada*

(Received 30 April 2012; published 26 June 2012)

We study Higgs-radion mixing in a warped extra-dimensional model with standard model fields in the bulk, and we include a fourth generation of chiral fermions. The main problem with the fourth generation is that, in the absence of Higgs-radion mixing, it produces a large enhancement in the Higgs production cross section, now severely constrained by LHC data. We analyze the production and decay rates of the two physical states emerging from the mixing and confront them with present LHC data. We show that the current signals observed can be compatible with the presence of one, or both, of these Higgs-radion mixed states (the ϕ and the h), although with a severely restricted parameter space. In particular, the radion interaction scale must be quite low, $\Lambda_\phi \sim$ 1–1.5 TeV. If $m_\phi \sim 125$ GeV, the h state must be heavier ($m_h > 320$). If $m_h \sim 125$ GeV, the ϕ state must be quite light or close in mass ($m_\phi \sim 120$ GeV). We also present the modified decay branching ratios of the mixed Higgs-radion states, including flavor-violating decays into fourth-generation quarks and leptons. The windows of allowed parameter space obtained are very sensitive to the increased precision of upcoming LHC data. During the present year, a clear picture of this scenario will emerge, either confirming or further severely constraining this scenario.

DOI: 10.1103/PhysRevD.85.115025 PACS numbers: 12.60.−i, 11.10.Kk, 14.80.−j

I. INTRODUCTION

While the sandard model (SM) is successful in explaining most, but not all, of the present experimental data, it suffers from theoretical inconsistencies. Outstanding amongst these are the two hierarchy problems: the discrepancy between the Planck and the electroweak scale, and the fermion mass hierarchy. Thus, it is generally expected that new physics around the TeV scale is needed to stabilize the Higgs mass and solve the hierarchy problem. Originally, warped extra-dimensional models were introduced to explain the first discrepancy [1]. In the original scenario, two branes are introduced, one with an energy scale set at the Planck scale, the other at the TeV scale, with the SM fields localized on the TeV brane, and with gravity allowed to propagate in the bulk. The exponential warp factor arising from the anti-de Sitter geometry accounts for the seemingly unnatural difference between the Planck and the electroweak scales.

Allowing SM fermions and gauge fields to propagate in the bulk [2] can also explain the fermion mass hierarchy by fermion localization [3,4]. One shortcoming of this minimal model is that the Kaluza-Klein (KK) excitations of the bulk have masses compatible with the compactification scale, and tight bounds from precision electroweak tests [5] and from flavor physics [6] constrain them to be in the few TeV range, an obstacle in producing and observing these resonances at the LHC.

The tests of the model would then likely come from observing other particles, in particular, the radion, which is a scalar field associated with fluctuations in the size of the extra dimension, and playing a role in its stabilization. In a simple model with a bulk scalar which generates a vacuum expectation value (VEV), the radion field emerges as a pseudo-Goldstone boson associated with the breaking of translation symmetry [7]. The advantage is that the mass of the radion does not depend on the compactification scale but only on the mechanism that stabilizes the size of the extra dimension. The radion couples to brane matter through the trace of the energy-momentum tensor; when matter propagates in the bulk the couplings receive some corrections [8] but the main component of the coupling remains proportional to the masses of the particles, in a similar fashion to the Higgs boson. In fact, as they share same quantum numbers, the radion field can mix with the Higgs boson after electroweak symmetry breaking, which involves another parameter, the coefficient of the curvature-scalar term [9]. Generically, the radion may be the lightest new state in a Randall-Sundrum-type setup, with a mass typically suppressed with respect to KK fields by a volume factor of ~40 [10], which then might put its mass between a few tens to hundreds of GeV, with suppressed couplings which allow it to have escaped detection at CERN LEP, and consistent with precision electroweak data.

The interest in scalar particles beyond the SM has been fueled by the recent ATLAS and CMS searches. Although clear evidence for a new state is at present inconclusive, there are exclusion regions reported by ATLAS [11]: 112.9 GeV $\leq m_{h^0} \leq$ 115.5 GeV, 131 GeV $\leq m_{h^0} \leq$ 238 GeV and 251 GeV $\leq m_{h^0} \leq$ 466 GeV at 95% C.L., while the mass region excluded by CMS [12] is 127 GeV $\leq m_{h^0} \leq$ 600 GeV at 95% C.L. In the meantime, both experiments observed an intriguing excess of

*mfrank@alcor.concordia.ca
†beste.korutlu@gmail.com
‡mtoharia@physics.concordia.ca

events for a possible Higgs boson with mass close to $m_{h^0} = 126$ GeV for ATLAS and 124 GeV for CMS. The three most sensitive channels in this mass range, $h^0 \to \gamma\gamma$, $h^0 \to ZZ^* \to l^+l^-l^+l^-$, and $h^0 \to WW^* \to l^+\nu l^-\bar{\nu}$ contribute to the excess with significances of 3.1σ, 2.1σ and 1.4σ, respectively. If this would be confirmed by further data analyses in 2012, a Higgs boson of mass around 125 GeV may be indicative of physics beyond the SM due to the vacuum instability [13]. Furthermore, the observed 3.1σ excess in the $\gamma\gamma$ channel observed by ATLAS is higher than the expected signals of the pure SM Higgs boson (with the same mass), which again points to new physics.

As the window for new physics opens, one can naturally ask if the new state is a Higgs, a radion, or a Higgs-radion mixed state. This possibility could have even more dramatic consequences for the scenario with an additional generation of fermions, which is a natural extension of the warped space model as in [14]. Reexamination of electroweak (EW) precision data showed that a fourth generation of fermions is not ruled out experimentally. Additionally, an extra generation was shown to have theoretically attractive features, and could help address some of the fundamental open questions, such as baryon asymmetry of the Universe, Higgs naturalness, fermion mass hierarchy, and dark matter (see [15] and for a recent review, [16] and references therein). However, at present four generations phenomenology may not be in such a good shape. There are increasing indications from CMS and ATLAS that the fourth-generation quarks would be very heavy [17], though all the tests have assumptions which may or may not hold. In any case, based basically on the enhancement of the Higgs production rate via $gg \to h^0$ in four generations (by a factor of 4–9), the ensuing enhancement of the decay $h^0 \to gg$, and the suppression of $h^0 \to \gamma\gamma$ the Higgs boson is excluded in the mass range 120–600 GeV at 95%, and in the range 125–600 GeV at 99% C.L. [18]. In particular, it appears that if the bump in the signal at CMS and LHC is the Higgs boson, this would rule out the SM4 at 95% confidence level for $m_{h^0} \geq 123$ GeV, and at 99.6% if $m_{h^0} = 125$ GeV [19]. The limits from the Tevatron [20] also exclude a wide range of Higgs boson masses.

In a recent study, we have shown that if the fourth generation is incorporated into the framework of warped space models, both the production and decay patterns of the Higgs bosons can be altered significantly with respect to the patterns expected in the standard model with four generations, thus giving rise to distinguishing signals at the colliders [21]. Radion phenomenology with and without Higgs-radion mixing has been discussed in several papers [8,22,23]. It has been shown that a tree-level misalignment between the flavor structure of the Yukawa couplings of the radion and the fermion mass matrix will appear when the fermion bulk parameters are not all degenerate in both three [24] and four generations [25]. In this last reference, it was also pointed out that the radion is less sensitive to the presence of an extra generation than the Higgs boson.

As the mechanism responsible for the radion flavor-changing neutral currents (FCNC's) is different from the one for the Higgs in these same models [26,27], and the branching ratios for decays into gluons and photons for three and four generations also differs, we can expect the phenomenology of the Higgs-radion mixed state to present an interesting interplay of the two mechanisms responsible, and to yield different effects. In particular, this mixing may help evade the apparent constraints on low Higgs masses in the four-generation scenario. Motivated by these expectations, we study the phenomenology of the Higgs-radion mixed state, paying particular attention to the signals for $gg \to \phi \to \gamma\gamma$, $gg \to \phi \to ZZ^*$, as well as $gg \to h \to \gamma\gamma$, $gg \to h \to ZZ^*$, where ϕ and h stand for the mixed Higgs-radion states. We use the presently available ATLAS [11] and CMS data [12] for scalar searches to identify regions in the parameter space where the data is compatible with one or the other of these states. Similar analysis with the mixing effects in three generations has been most recently studied in [28]. In SM4, the new quarks and leptons are expected to be very heavy. CMS sets a stringent bound, $m_{t'} > 557$ GeV [29] assuming that $t' \to Wb$ has a branching ratio of 1, while ATLAS sets a lower bound $m_{t'} > 404$ GeV from $t'\bar{t}' \to WbW\bar{b}$ [30]. For b', the limit is $m_{b'} > 450$ GeV from ATLAS [31], assuming 100% decay $b' \to Wt$. These limits do not necessarily apply to our model where significant FCNC decays $t' \to Zt$, Ht and $b' \to Zb$, Hb are expected [21], with a nondiagonal CKM matrix for 4 generations.

Our paper is organized as follows. In the next section (Sec. II), we briefly review the warped model with fermions in the bulk. We then discuss the production and decays of the Higgs-radion mixed states (Sec. III) and discuss regions of the parameter space where the events at the LHC would be compatible with observing a mixed state. For the allowed parameter space, we present the flavor-changing and flavor-violating decays of the two Higgs-radion states in Sec. IV. We take throughout $m_{t'} = 400$ GeV, $m_{b'} = 350$ GeV, and $m_{\nu'} = 90$ GeV and analyze cases in which the fourth-generation charged lepton mass is $m_{\tau'} = 150$ GeV, or a lighter $m_{\tau'} = 100$ GeV, as its mass has important implications in the Higgs branching ratios. We summarize our findings and conclude in Sec. V.

II. THE MODEL

The anti-de Sitter metric including the scalar perturbation F is given in the Randall-Sundrum coordinate system by [32]

$$ds^2 = e^{-2(A+F)}\eta_{\mu\nu}dx^\mu dx^\nu - (1+2F)^2 dy^2 = \left(\frac{R}{z}\right)^2 (e^{-2F}\eta_{\mu\nu}dx^\mu dx^\nu - (1+2F)^2 dz^2), \quad (1)$$

where $A(y) = ky$. The radion graviscalar is the scalar component of the five-dimensional (5D) gravitational perturbations and tracks fluctuations of the size of the extra-dimension (i.e. its "radius"). The perturbed metric is no longer conformally flat, and in linear order in the fluctuation F, the metric perturbation is given by

$$\delta(ds^2) \approx -2F(e^{-2A}\eta_{\mu\nu}dx^\mu dx^\nu + 2dy^2) = -2F\left(\frac{R}{z}\right)^2(\eta_{\mu\nu}dx^\mu dx^\nu + 2dz^2), \quad (2)$$

where $F(z, x)$ is the 5D radion field. The radion acquires mass through a stabilization mechanism with the addition of a bulk scalar field with a VEV, which, after taking into account the backreaction of the geometry due to the scalar field VEV profile [10], leads to an effective potential for the radion. We assume that this backreaction is small, and does not have a large effect on the 5D profile of the radion.

The relation between the canonically normalized four-dimensional radion field $\phi_0(x)$ and the metric perturbation $F(z, x)$ is given by

$$F(z, x) = \frac{1}{\sqrt{6}}\frac{R^2}{R'}\left(\frac{z}{R}\right)^2\phi_0(x) = \frac{\phi_0(x)}{\Lambda_\phi}\left(\frac{z}{R'}\right)^2, \quad (3)$$

where $\Lambda_\phi = \sqrt{6}M_{\rm Pl}e^{-ky_{\rm IR}}$ is the radion interaction scale.[1] We take the value of k as $\sim M_5$, and $\Lambda_\phi \sim e^{-kL}M_5$ is expected to be ~TeV. In the warped model with SM fields propagating in the bulk, radion interactions with SM matter are slightly modified with respect to the case of the SM lying on the TeV brane [8]. But still, they remain quite similar in form to the interactions of SM Higgs except for an overall proportional constant, the inverse of the radion interaction scale Λ_ϕ. The radion effective interaction Lagrangian yields the following coupling to gluons (QCD) and photons (EM):

$$\mathcal{L}_{g,A} = -\frac{\phi_0}{4\Lambda_\phi}\Big\{\Big[\frac{1}{kL}[1 - 4\pi\alpha_s(\tau_{\rm UV} + \tau_{\rm IR})] + \frac{\alpha_s}{2\pi}\Big(b_{\rm QCD} - \frac{1}{2}F_{1/2}(\tau_t)\Big)\Big]\sum_a G^a_{\mu\nu}G^{a\mu\nu} + \Big[\frac{1}{kL}[1 - 4\pi\alpha(\tau_{\rm UV} + \tau_{\rm IR})] + \frac{\alpha}{2\pi}\Big(b_{\rm EM} - F_1(\tau_W) - \frac{4}{3}F_{1/2}(\tau_t)\Big)\Big]F_{\mu\nu}F^{\mu\nu}\Big\}. \quad (4)$$

The radion couplings to W and Z bosons are

$$\mathcal{L}_V = -\frac{2\phi_0}{\Lambda_\phi}\Big[\Big(\mu_W^2 W^+_\mu W^{-\mu} + \frac{1}{4kL}W^\dagger_{\mu\nu}W^{\mu\nu}\Big) + \Big(\frac{\mu_Z^2}{2}Z_\mu Z^\mu + \frac{1}{8kL}Z_{\mu\nu}Z^{\mu\nu}\Big)\Big], \quad (5)$$

where $V_{\mu\nu} = \partial_\mu V_\nu - \partial_\nu V_\mu$ for $V_\mu = W^\pm_\mu$, Z_μ and μ_i^2 ($i = W, Z$) include the contributions from the bulk wave functions of W, Z, and are given as a function of the W and Z mass $m_{W,Z}$ $\mu_i^2 = m_i^2[1 - \frac{kL}{2}(\frac{m_i}{k})^2]$.

The radion couplings to quarks (similar results hold for leptons) are proportional to their masses:

$$\mathcal{L}_f = -\frac{\phi_0(x)}{\Lambda_\phi}(q^i_L u^j_R + \bar{q}^i_L \bar{u}^j_R)m^u_{ij}[\mathcal{I}(c_{q_i}) + \mathcal{I}(c_{u_j})] + (u \to d), \quad (6)$$

where $\frac{c_{q_i}}{R}$, $\frac{c_{u_i}}{R}$ and $\frac{c_{d_i}}{R}$ are the 5D fermion masses, and we choose to work in the basis where these are diagonal in 5D flavor space. $\mathcal{I}(c)$ is obtained as

$$\mathcal{I}(c) = \left[\frac{(\frac{1}{2} - c)}{1 - (R/R')^{1-2c}} + c\right] \approx \begin{cases} c & (c > 1/2) \\ \frac{1}{2} & (c < 1/2) \end{cases}. \quad (7)$$

This result was first obtained for the case of a brane Higgs and a single family of fermions in [8], and it was later generalized to three families and bulk Higgs in [24], where it was noted that these couplings lead to flavor violation in the interactions between the radion and fermions.

Since the radion and the Higgs bosons have the same quantum numbers, it is possible for them to mix via kinetic factors:[2]

$$S_\xi = \xi\int d^4x\sqrt{-g_{\rm vis}}R(g_{\rm vis})\hat{H}^\dagger\hat{H}, \quad (8)$$

with $R(g)$ the Ricci scalar. The effective four-dimensional Lagrangian up to quadratic order will be

$$\mathcal{L} = -\tfrac{1}{2}(1 + 6\gamma^2\xi)\phi_0\Box\phi_0 - \tfrac{1}{2}\phi_0 m^2_{\phi_0}\phi_0 - \tfrac{1}{2}h_0(\Box + m^2_{h_0})h_0 - 6\gamma\xi\phi_0\Box h_0, \quad (9)$$

where m_{h_0} and m_{ϕ_0} are the Higgs and radion masses before mixing. After rescaling to obtain states that diagonalize the kinetic and the mass terms (following [23])

$$h_0 = (\cos\theta - 6\xi\gamma/Z\sin\theta)h + (\sin\theta + 6\xi\gamma Z\cos\theta)\phi \equiv dh + c\phi, \quad (10)$$

$$\phi_0 = -\cos\theta\frac{\phi}{Z} + \sin\theta\frac{h}{Z} \equiv a\phi + bh, \quad (11)$$

[1]This relation of Λ_ϕ could be slightly modified with the addition of gravity brane kinetic terms on the IR brane, and thus allow some flexibility on the precise definition of Λ_ϕ in terms of the other model parameters.

[2]We note that in the case of a bulk Higgs, there will be Higgs-radion mixing at the level of the bulk scalar potential, without the need to introduce kinetic mixing. For simplicity, we will assume that the Higgs is highly localized on the brane and consider only brane kinetic mixing.

with the mixing angle θ defined as

$$\tan 2\theta = 12\gamma\xi Z \frac{m_{h_0}^2}{m_{\phi_0}^2 - m_{h_0}^2 (Z^2 - 36\xi^2\gamma^2)}, \quad (12)$$

where $Z^2 = 1 + 6\xi\gamma^2(1 - 6\xi) = \beta - 36\xi^2\gamma^2$. The requirement $Z^2 > 0$, which in turn gives $\beta > 0$, is needed to maintain positive-definite kinetic terms for the physical fields h and ϕ. This requirement brings theoretical limits on the ξ parameter, which describes the mixing between the Higgs and radion states, such that

$$\frac{1}{12}\left(1 - \sqrt{1 + \frac{4}{\gamma^2}}\right) \le \xi \le \frac{1}{12}\left(1 + \sqrt{1 + \frac{4}{\gamma^2}}\right). \quad (13)$$

The parameter ξ is also subject to strong restrictions coming from precision electroweak constraints (on S and T parameters), LEP/LEP2 data, and Tevatron bounds [10,33]. In addition, there are theoretically excluded parameter regions which do not satisfy requirements of $m_h - m_\phi$ degeneracy. The mass squared values for the physical states are obtained as

$$m_\pm^2 = \frac{1}{2Z^2}\Big(m_{\phi_0^2} + \beta m_{h_0}^2 \pm \sqrt{(m_{\phi_0^2} + \beta m_{h_0}^2)^2 - 4Z^2 m_{\phi_0^2} m_{h_0}^2}\Big), \quad (14)$$

where the larger(smaller) of m_h and m_ϕ will be identified as $m_+(m_-)$, and these must satisfy the inequality

$$\frac{m_+^2}{m_-^2} > 1 + \frac{2\beta}{Z^2}\left(1 - \frac{Z^2}{\beta}\right) + \frac{2\beta}{Z^2}\left(1 - \frac{Z^2}{\beta}\right)^{1/2}, \quad (15)$$

to keep the bare masses real.

The presence of mixing will modify the couplings to fermions, gluons, photons, $W's$ and $Z's$ of both the radion and the Higgs boson and thus change the corresponding decay branching ratios as well as the production rates.

III. PRODUCTION AND DECAYS OF A MIXED HIGGS-RADION STATE WITH FOUR GENERATIONS

The main production mechanism of the Higgs particles at the hadron colliders is through the gluon-gluon fusion channel, $\sigma(gg \to h_{SM})$, via triangular loops of heavy quarks. However, for heavier Higgs bosons, the weak vector boson fusion channel, $\sigma(qq \to qqh_{SM})$, becomes competitive with the gluon-gluon fusion mode. Therefore, as a good approximation one can write the ratio of the production cross section of the h physical mode to the production cross section of SM Higgs as $\frac{\sigma(gg\to h)+\sigma(qq\to qqh)}{\sigma(gg\to h_{SM})+\sigma(qq\to qqh_{SM})}$, and this becomes

$$\frac{\sigma(gg\to h)+\sigma(qq\to qqh)}{\sigma(gg\to h_{SM})+\sigma(qq\to qqh_{SM})} = \left(\frac{\sigma(gg\to h)}{\sigma(gg\to h_{SM})} + \frac{\sigma(qq\to qqh)}{\sigma(gg\to h_{SM})}\right)\left(\frac{1}{1+\frac{\sigma(qq\to qqh_{SM})}{\sigma(gg\to h_{SM})}}\right). \quad (16)$$

The ratio of the Higgs production cross section via the weak vector boson fusion channel to the production cross section of the SM Higgs is closely correlated with the partial widths such that

$$\frac{\sigma(qq\to qqh)}{\sigma(qq\to qqh_{SM})} = \frac{\Gamma(h\to WW)}{\Gamma(h_{SM}\to WW)}, \quad (17)$$

which in warped extra-dimensional scenarios with Higgs-radion mixing and fields in the bulk simply becomes

$$\frac{\Gamma(h\to WW)}{\Gamma(h_{SM}\to WW)} = \left(d + b\gamma\left(1 - 3\ln\left(\frac{\sqrt{6}M_{Pl}}{\Lambda_\phi}\right)\frac{M_W^2}{\Lambda_\phi^2}\right)\right)^2. \quad (18)$$

Substituting this result in Eq. (16) we obtain, for the right-hand side,

$$\left[\frac{\sigma(gg\to h)}{\sigma(gg\to h_{SM})} + \left(d + b\gamma\left(1 - 3\ln\left(\frac{\sqrt{6}M_{Pl}}{\Lambda_\phi}\right)\frac{M_W^2}{\Lambda_\phi^2}\right)\right)^2 \times \frac{\sigma(qq\to qqh_{SM})}{\sigma(gg\to h_{SM})}\right]\left(\frac{1}{1+\frac{\sigma(qq\to qqh_{SM})}{\sigma(gg\to h_{SM})}}\right), \quad (19)$$

where the first term in the brackets is simply the ratio of couplings to gluons $c_g^2/c_{g_{SM}}^2$.

Similarly, we can calculate the same ratio for the field ϕ,

$$\left[\frac{\sigma(gg\to \phi)}{\sigma(gg\to h_{SM})} + \left(c + a\gamma\left(1 - 3\ln\left(\frac{\sqrt{6}M_{Pl}}{\Lambda_\phi}\right)\frac{M_W^2}{\Lambda_\phi^2}\right)\right)^2 \times \frac{\sigma(qq\to qqh_{SM})}{\sigma(gg\to h_{SM})}\right]\left(\frac{1}{1+\frac{\sigma(qq\to qqh_{SM})}{\sigma(gg\to h_{SM})}}\right). \quad (20)$$

The production mechanism of an unmixed Higgs boson through the gluon-gluon fusion channel increases about 9 times with an additional fourth family of fermions, because in addition to the top quark there are also heavy t' and b' quarks propagating in the loop. Recently, the two-loop EW corrections, δ_{EW}^4, to the Higgs boson production via gluon-gluon fusion has been computed with respect to the leading-order cross section in [34–37]

$$\sigma_{SM4}(gg\to h_0) = \sigma_{SM4}^{LO}(gg\to h_0)(1 + \delta_{EW}^4). \quad (21)$$

This enters as a correction to the Higgs field prior to mixing. For δ_{EW}^4, we have taken the (Higgs-mass-dependent) values from Table I in [37].

Also, in order to take into account the effects of KK fields in the loop, we assume an additional correction to the h_0 couplings squared to massless gauge bosons of $\pm 20\%$ for gluons and $\pm 10\%$ for photons. The estimated values of

TABLE I. The FCNC branching ratios of h and ϕ for allowed points in the parameter space. The fourth-generation fermion masses are chosen as $m_{t'} = 400$ GeV, $m_{b'} = 350$ GeV, $m_{\tau'} = 100$ GeV, $m_{\nu_{\tau'}} = 90$ GeV.

Λ(TeV)	ξ	m(GeV)	$b'b$	tc	bs	$\tau'\tau$	$\mu\tau$	$\nu_\tau\nu_{\tau'}$
1.3	0.228	$m_\phi = 60$	$\cdots$	$\cdots$	9.53×10^{-5}	$\cdots$	2.49×10^{-5}	$\cdots$
		$m_h = 125$	$\cdots$	$\cdots$	5.51×10^{-4}	5.53×10^{-1}	1.52×10^{-4}	1.46×10^{-3}
1.3	−0.008 66	$m_\phi = 124$	$\cdots$	$\cdots$	7.30×10^{-5}	4.67×10^{-2}	2.01×10^{-5}	7.76×10^{-4}
		$m_h = 120$	$\cdots$	$\cdots$	6.34×10^{-4}	4.74×10^{-1}	1.77×10^{-4}	1.48×10^{-3}
1.5	0.0221	$m_\phi = 120$	$\cdots$	$\cdots$	3.31×10^{-4}	2.20×10^{-1}	9.06×10^{-5}	1.46×10^{-3}
		$m_h = 124$	$\cdots$	$\cdots$	7.34×10^{-4}	7.19×10^{-1}	2.02×10^{-4}	1.76×10^{-3}
1.0	0.417	$m_\phi = 125$	$\cdots$	$\cdots$	7.47×10^{-5}	5.94×10^{-2}	2.05×10^{-5}	8.15×10^{-4}
		$m_h = 320$	$\cdots$	1.53×10^{-4}	1.04×10^{-6}	7.84×10^{-3}	3.23×10^{-7}	9.28×10^{-6}
1.0	0.537	$m_\phi = 125$	$\cdots$	$\cdots$	4.21×10^{-5}	2.95×10^{-3}	1.16×10^{-5}	6.92×10^{-4}
		$m_h = 500$	1.27×10^{-2}	6.61×10^{-5}	2.93×10^{-7}	2.71×10^{-3}	9.83×10^{-8}	3.00×10^{-6}
1.0	0.601	$m_\phi = 125$	$\cdots$	$\cdots$	1.52×10^{-5}	7.29×10^{-3}	4.17×10^{-6}	5.42×10^{-4}
		$m_h = 600$	1.44×10^{-2}	4.84×10^{-5}	1.99×10^{-7}	1.89×10^{-3}	6.68×10^{-8}	2.02×10^{-6}

the corrections are based on the results presented in [38], where it was shown that either enhancements or suppressions in the rates are possible, depending on the phases present at the level of the 5D Yukawa couplings. In the figures, the effect will be illustrated with bands in parameter space representing this "theoretical uncertainty (THU)."

With these considerations, the gg and $\gamma\gamma$ couplings of the physical Higgs and radion fields become

$$\begin{aligned} c_g^{h,\phi}(\max) &= -\frac{\alpha_s}{4\pi v}\Big[g_g^{h,\phi}(\max)\sum_i F_{1/2}(\tau_i) \\ &\quad - 2\Big(b_3' + \frac{2\pi}{\alpha_s \ln(\frac{\sqrt{6}M_{\rm Pl}}{\Lambda_\phi})}\Big)g^{h,\phi}\Big], \\ c_g^{h,\phi}(\min) &= -\frac{\alpha_s}{4\pi v}\Big[g_g^{h,\phi}(\min)\sum_i F_{1/2}(\tau_i) \\ &\quad - 2\Big(b_3' + \frac{2\pi}{\alpha_s \ln(\frac{\sqrt{6}M_{\rm Pl}}{\Lambda_\phi})}\Big)g^{h,\phi}\Big], \\ c_\gamma^{h,\phi}(\max) &= -\frac{\alpha}{2\pi v}\Big[g_\gamma^{h,\phi}(\max)\sum_i e_i^2 N_c^i F_i(\tau_i) \\ &\quad - \Big(b_2' + b_Y' + \frac{2\pi}{\alpha \ln(\frac{\sqrt{6}M_{\rm Pl}}{\Lambda_\phi})}\Big)g^{h,\phi}\Big], \\ c_\gamma^{h,\phi}(\min) &= -\frac{\alpha}{2\pi v}\Big[g_\gamma^{h,\phi}(\min)\sum_i e_i^2 N_c^i F_i(\tau_i) \\ &\quad - \Big(b_2' + b_Y' + \frac{2\pi}{\alpha \ln(\frac{\sqrt{6}M_{\rm Pl}}{\Lambda_\phi})}\Big)g^{h,\phi}\Big], \end{aligned} \tag{22}$$

where b_3', b_2' and b_Y' are the coefficients of the beta functions of the $SU(3)$, $SU(2)$ and $U(1)_Y$ groups, respectively, in the presence of 4 generations of quarks and leptons. The coefficients are $b_3' = 18/3$ and $b_2' + b_Y' = -65/9$. The loop functions $F_{1/2}$ and F_i are standard, as defined, for example, in [39], and their numerical value depends on whether the fourth-generation quarks are heavier or lighter than the scalar in question (h or ϕ). The index i indicates a sum over the top quark and the fourth-generation fermions. Also, we have defined

$$\begin{aligned} g_g^\phi(\max) &= a\gamma + c\sqrt{(1+\delta_{\rm EW}^4)(1.20)}, \\ g_\gamma^\phi(\max) &= a\gamma + c\sqrt{(1.10)(1+\bar\delta_{\rm EW}^4)(1+\delta_{\rm THU})}, \\ g_g^h(\max) &= b\gamma + d\sqrt{(1+\delta_{\rm EW}^4)(1.20)}, \\ g_\gamma^h(\max) &= b\gamma + d\sqrt{(1.10)(1+\bar\delta_{\rm EW}^4)(1+\delta_{\rm THU})}, \\ g_g^\phi(\min) &= a\gamma + c\sqrt{(1+\delta_{\rm EW}^4)(0.80)}, \\ g_\gamma^\phi(\min) &= a\gamma + c\sqrt{(0.90)(1+\bar\delta_{\rm EW}^4)(1-\delta_{\rm THU})}, \\ g_g^h(\min) &= b\gamma + d\sqrt{(1+\delta_{\rm EW}^4)(0.80)}, \\ g_\gamma^h(\min) &= b\gamma + d\sqrt{(0.90)(1+\bar\delta_{\rm EW}^4)(1-\delta_{\rm THU})}, \\ g^\phi &= a\gamma, \qquad g^h = b\gamma. \end{aligned} \tag{23}$$

Note that while the bare Higgs (h_0) couplings are corrected by $(1+\delta_{\rm EW}^4)$, there is no such correction for the bare radion (ϕ_0) couplings. The reason is that the latter are dominated by the trace anomaly, and so higher-order loop effects are much smaller. We have also included the corrections to the $h_0 \to \gamma\gamma$ coupling due to loop effects, as given in Table 3 of [37]. A note of caution is warranted with these corrections. The authors show that the next-to-leading order EW corrections are of the same order as the leading-order (LO) estimate, and negative, due to the strong cancellation between the W and fermion loops with four generations. This might be indicative of a nonperturbative regime, and the authors rely on an estimation of the higher-order corrections, without any certainty that the perturbation series converges. Moreover, in our scenario, heavy Kaluza-Klein fermions are known to affect $h_0 \to \gamma\gamma$ at lowest order [38,40], and therefore any higher-order correction should also include the effect of heavy fermions, not present in SM4. Given these uncertainties, we will present the figures for both LO and EW-corrected branching ratios (BRs) to $\gamma\gamma$, expressed as in [37], and comment on the differences. We mostly focus on the decays of Higgs-radion mixed states to $\gamma\gamma$ and ZZ^* for the low mass region, and to ZZ channel for larger masses. The ratio of discovery significances for both the h and the ϕ with respect to the SM Higgs can be defined as

$$R_h(XX) = \left[\frac{\sigma(gg \to h) + \sigma(qq \to qqh)}{\sigma(gg \to h_{\rm SM}) + \sigma(qq \to qqh_{\rm SM})}\right] \times \frac{{\rm BR}(h \to XX)}{{\rm BR}(h_{\rm SM} \to XX)} w_{\rm corr}(h), \tag{24}$$

and

$$R_\phi(XX) = \left[\frac{\sigma(gg \to \phi) + \sigma(qq \to qq\phi)}{\sigma(gg \to h_{\rm SM}) + \sigma(qq \to qqh_{\rm SM})}\right] \times \frac{{\rm BR}(\phi \to XX)}{{\rm BR}(h_{\rm SM} \to XX)} w_{\rm corr}(\phi), \tag{25}$$

where the terms in square brackets are defined in Eqs. (19) and (20) and where

$$w_{\rm corr}(s) = \begin{cases} \sqrt{\frac{\max(\Gamma_{\rm tot}(h_{\rm SM}), \Delta M_{4l})}{\max(\Gamma_{\rm tot}(s), \Delta M_{4l})}} & \text{for } \Gamma_{\rm tot}(s) > \Gamma_{\rm tot}(h_{\rm SM}) \\ 1 & \text{for } \Gamma_{\rm tot}(s) < \Gamma_{\rm tot}(h_{\rm SM}). \end{cases} \tag{26}$$

The term $w_{\rm corr}$ represents a crude and fast approximation of the effects of a large width of either $s = h$ or $s = \phi$. Indeed, if the physical state h (or ϕ) has a much larger width than the SM Higgs, and if this width is larger than the experimental resolution of the detector, then an LHC search looking for the SM Higgs would somewhat underestimate the integrated signal as this one would be distributed in a much wider resonance. We have checked numerically using a Breit-Wigner distribution shape that the correction induced indeed scales roughly as in $w_{\rm corr}$, which was originally introduced as a width-effect correction for the radion in [9].

Finally, the experimental resolution in the 4-lepton channel is estimated to be [9]

$$\frac{\Delta M_{4l}}{M_{4l}} = \frac{0.1}{\sqrt{M_{4l}({\rm GeV})}} + 0.005. \tag{27}$$

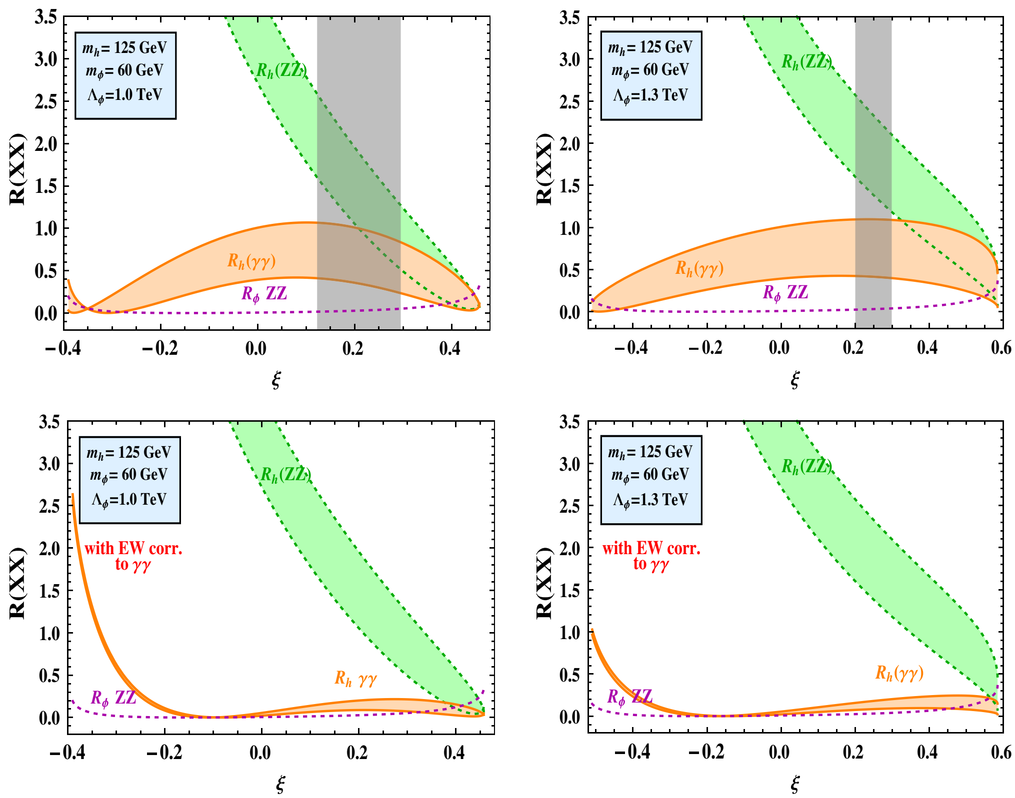

FIG. 1 (color online). Ratio of discovery significances $R(XX) \sim \sigma/\sigma_{\rm SM}$, defined in the text, for $m_h = 125$ GeV, $m_\phi = 60$ GeV and for different values of Λ_ϕ and $m_{\tau'}$, for $m_{\tau'} = 100$ GeV. In the upper panels we show the LO, and in the lower panels the EW-corrected branching ratio to $\gamma\gamma$. The light green bands indicate the theoretical uncertainties in the $gg \to h \to ZZ^*$ rate, while those for $\gamma\gamma$ are depicted in orange. The dashed purple lines marked by $R_\phi(ZZ)$ indicate the ratio of $\phi Z^* Z^*$ couplings with respect to the $h_{\rm SM} Z^* Z^*$ one. The vertical gray bands indicate the allowed parameter space for ξ.

We use all this information to explore the parameter space for m_ϕ and m_h consistent with the LHC data, which indicates an excess in the mass region 120–128 GeV.

We review the data so far. ATLAS data indicates an enhanced signal in $\gamma\gamma$ and $ZZ^* \to 4\ell$ near 125 GeV [11] with observed excesses: $R(\gamma\gamma) = 2^{+0.8}_{-0.8}$, $R(4\ell) = 0.5^{+1.5}_{-0.5}$.

CMS data [12] indicates an excess at 124 GeV: $R(\gamma\gamma) = 1.7^{+0.8}_{-0.7}$, $R(4\ell) = 0.5^{+1.1}_{-0.5}$, $R(b\bar{b}) = 1.2^{+2.0}_{-1.2}$ and possibly an additional enhancement either at 120 GeV in ZZ^* only: $R(4\ell) = 2^{+1.5}_{-1}$, $R(b\bar{b}) = 0.2^{+1.9}_{-0.2}$, while $R(\gamma\gamma) < 0.5$, or at 137 GeV in $\gamma\gamma$, $R(\gamma\gamma) = 1.5^{+0.8}_{-0.8}$ but not in ZZ^*, $R(4\ell) < 0.2$. The errors bars on the data are still large, but they can be used to restrict the parameter for the four-generation Higgs-radion mixed states. In order for these states to fit the data, we should either have one of the states at 124–126 GeV, and another one hidden (i.e. below the LHC signal), or one state at 124 GeV and the other either at 120 or 137 GeV, both which should respect the CMS signal characteristics. Additionally, from the plots we inferred the additional constraints for heavier Higgs bosons, which we used in generating our graphs: for $m_h = 320$ GeV, $R(ZZ) < 0.5$; for $m_h = 400$ GeV, $R(ZZ) < 0.2$; for $m_h = 500$ GeV, $R(ZZ) < 0.5$; and for $m_h = 600$ GeV, $R(ZZ) < 0.95$.

Based on the experimental constraints, we investigate the production and decay of the two scalar particles in our scenario, m_ϕ and m_h, and divide the parameter space as follows. In the first scenario, we attempt to fit h as the scalar particle observed at LHC at an invariant mass of $\sim$125 GeV, while requiring ϕ to be consistent with constraints of the rest of the spectrum from LEP, Tevatron and/or LHC; while in the second scenario, we attempt the same thing for ϕ, while h must be consistent with the previous collider data.

(i) Scenario 1a: $m_h = 124$ GeV, m_ϕ light (< 300 GeV); in particular, paying specific attention to $m_\phi = 120$ GeV, $m_\phi = 137$ GeV, as these seem possible parameter space points for the CMS data.

(ii) Scenario 1b: $m_h = 125$ GeV, m_ϕ heavy (> 300 GeV).

(iii) Scenario 2a: $m_\phi = 125$ GeV, m_h light (< 300 GeV); in particular, paying specific attention to the point $m_h = 120$ GeV.

(iv) Scenario 2b: $m_\phi = 125$ GeV, m_h heavy (> 300 GeV).

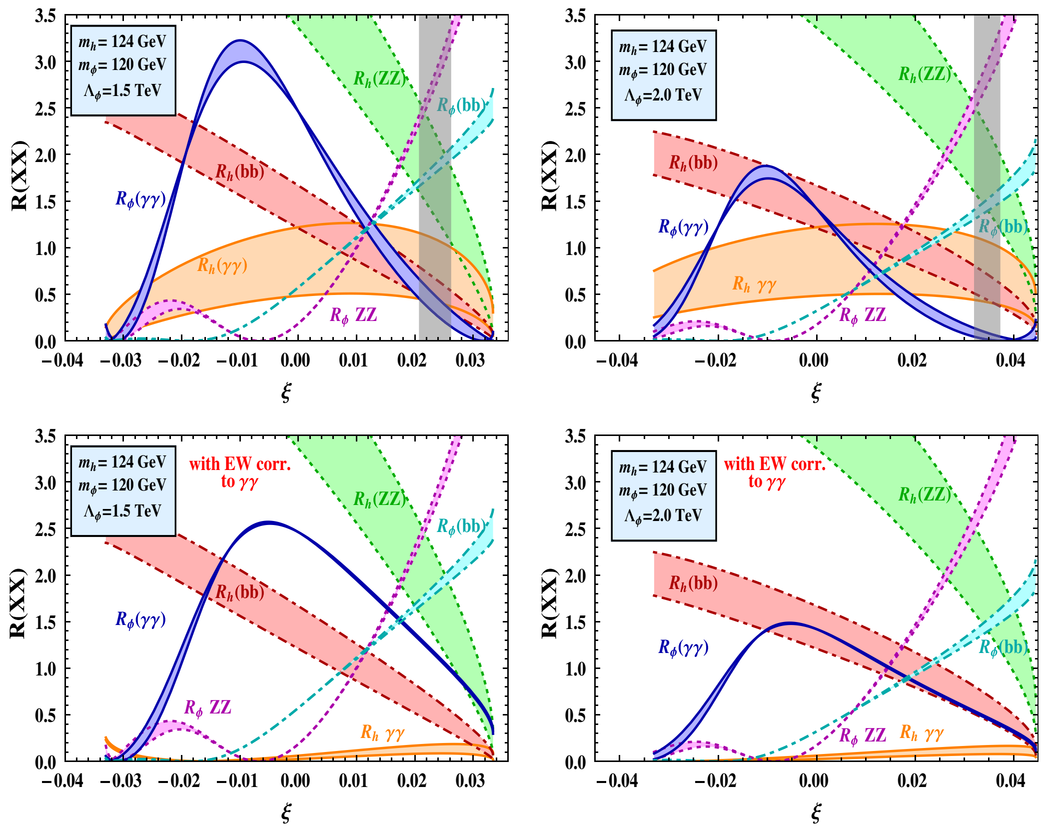

FIG. 2 (color online). Ratio of discovery significances $R(XX) \sim \sigma/\sigma_{SM}$, defined in the text, for $m_h = 124$ GeV, $m_\phi = 120$, $m_{\tau'} = 100$ GeV and for different values of Λ_ϕ. In the upper panels we show the LO, and in the lower panel the EW-corrected branching ratio to $\gamma\gamma$. The light green bands indicate the theoretical uncertainties in the ZZ^* signal, red for $b\bar{b}$ and orange for $\gamma\gamma$. For ϕ, the uncertainties are depicted in pink for ZZ^*, light blue for $b\bar{b}$ and purple for $\gamma\gamma$. The vertical gray bands indicate the allowed parameter space for ξ.

We illustrate some regions of parameter space with different masses of h and ϕ in the following figures. The results will depend on the mass of the fourth family charged lepton (τ') and so we divide our considerations into two parts. We first assume that $m_{\tau'} \geq 150$ GeV, thus preventing flavor-changing decays into $\tau'\tau$, which are potentially large in this model [21,25]. However, if the τ' is light, this might modify substantially the branching ratios, potentially yielding significantly different signals We comment on this case in this section, and investigate it in more detail in the next section.

(i) For Scenario 1a, if $m_\phi \leq 100$ GeV, the LEP and Tevatron constraints apply. We find that, constraining $R_\phi(Z^*Z^*)$ to be in the required range (< 0.5) forces $\xi < 0.3$ and $R_h(ZZ^*) < 1.6$. If we do not take into account the higher-order EW corrections to the $h\gamma\gamma$ coupling, we found that for $m_\phi = 60$ GeV the experimental constraints (including LEP) are satisfied for $\Lambda_\phi = 1.0$ TeV if $m_{\tau'} = 150$ GeV, and for $\Lambda_\phi = 1.0$, 1.3 TeV if $m_{\tau'} = 100$ GeV, as shown in the upper panel of Fig. 1. The tight LEP constraints on the $\Lambda_\phi - \xi$ parameter space disallow greater values of Λ_ϕ in the very light m_ϕ parameter region. However, when the large EW corrections to the $\gamma\gamma$ channel are included, we find no regions allowed anymore in this scenario (lower panel of Fig. 1). However, if $m_\phi = 120$ GeV, there exist points in the parameter space still consistent with all the experimental data for light τ' leptons. As both of the h and ϕ states are light, we graph the decays to $\gamma\gamma$, $b\bar{b}$ and ZZ^*. This parameter point is a point in the CMS data, and may or may not survive the latest round of data analysis. As both Higgs-radion mixed states are light, their branching ratios will depend on the τ' mass. If $m_{\tau'} = 100$ GeV, ϕ can decay into $\tau'\tau$, and the branching ratios to $b\bar{b}$, ZZ^* and $\gamma\gamma$ are modified. We present these in Fig. 2 for $\Lambda_\phi = 1.5$ and 2 TeV. From the figure (upper panels) one can note that, not including higher-order EW corrections to $\gamma\gamma$, there exist allowed regions of the parameter space. Again in this scenario, if we include EW corrections to $\gamma\gamma$ (lower panels) all allowed region disappear due to the reduced branching into $\gamma\gamma$. If $m_h = 124$ GeV, $m_\phi = 137$ GeV, we are unable to find points in the parameter space which satisfy the experimental constraints, with or without higher-order EW corrections to $\gamma\gamma$. If $R_\phi(ZZ^*) < 0.2$ as required,

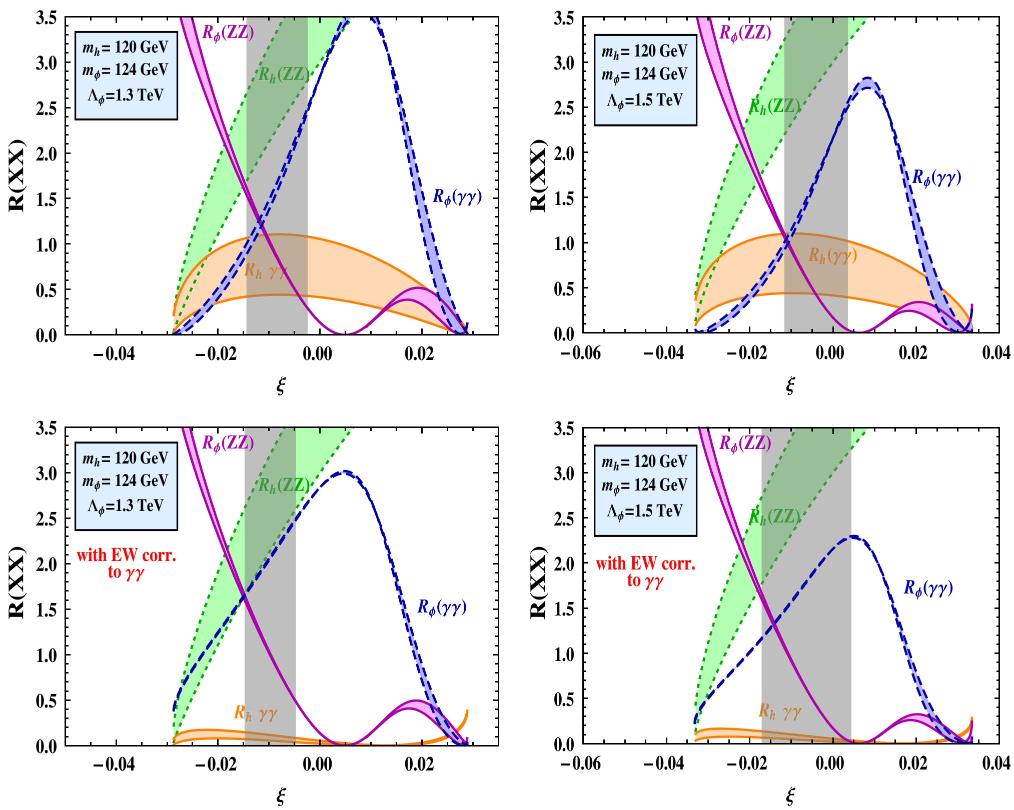

FIG. 3 (color online). Ratio of discovery significances $R(XX) \sim \sigma/\sigma_{\rm SM}$, defined in the text, for $m_h = 120$ GeV, $m_\phi = 125$ GeV and for different values of Λ_ϕ, for $m_{\tau'} = 100$ GeV. In the upper panels we show the LO, and in the lower panel the EW-corrected branching ratio to $\gamma\gamma$. The light green bands indicate the theoretical uncertainties in the ZZ^* signal and the orange the ones are for $\gamma\gamma$. For the ϕ, the theoretical uncertainties in ZZ^* are given by pink bands and the ones for $\gamma\gamma$ are in purple. The vertical gray bands indicate the allowed parameter space for ξ.

$R_\phi(\gamma\gamma) > 2.3$, and $R_h(ZZ^*) < 1.6$ for $\Lambda_\phi = 1$, 1.3, 1.5 TeV, and the branching ratios worsen for higher Λ_ϕ.

(ii) For Scenario 1b, increasing m_ϕ only makes the situation worse and we do not find any region of parameters in which an h state at 125 GeV and a heavy ϕ are allowed by the branching ratio constraints, and we thus choose not to show any figure for this case. We have so far found that only Scenario 1a allows some regions of parameter space, but with a very restrictive Λ_ϕ, and only if we do not consider the large suppressions in the $\gamma\gamma$ channel due to higher-order EW corrections.

(iii) In Scenario 2a, where $m_\phi = 124$ GeV and h is light, and for $m_{\tau'} = 150$ GeV, we do not find any allowed region in which all bounds and observed signals are respected. For regions where $R_h(\gamma\gamma) < 0.5$, $R_\phi(ZZ^*) < 1.6$. However, if the fourth-generation charged lepton τ' is light enough for the Higgs-radion mixed state(s) to decay into it (through flavor-violating decays $\tau\tau'$), the branching ratios are modified and the parameter space can shift. We show this in Fig. 3, for $m_h = 120$ GeV, $m_\phi = 124$ GeV and $\Lambda_\phi = 1.3$ TeV and $\Lambda_\phi = 1.5$ TeV. For $m_{\tau'} = 100$ GeV, the possibility of decays into $\tau\tau'$ reduces the branching ratios to the other channels, thus widening the allowed ξ parameter range and of Λ_ϕ for the Higgs-radion states. On the upper panels, we do not include higher-order corrections to $\gamma\gamma$ whereas these are taken into account in the lower panels. One can see that the reduction in $h \to \gamma\gamma$ due to these corrections enhances somewhat the allowed region since the reduction in $\gamma\gamma$ happens mostly for the h scalar, and this is preferred for its chosen mass of $m_h = 120$ GeV.

(iv) In Scenario 2b, we find that as long as h is heavy enough, there are regions of parameter space where all experimental constraints are satisfied. This is true independent of whether $m_{\tau'} = 100$ or 150 GeV, and also of whether one includes the higher-order EW corrections to $\gamma\gamma$. However, the results are quite sensitive to the value of Λ_ϕ and to the large experimental and theoretical uncertainties in the rates. We illustrate the situation for two values of Λ_ϕ, i.e $\Lambda_\phi = 1$ TeV in Fig. 4 and for $\Lambda_\phi = 1.3$ TeV in Fig. 5, for different h masses $m_h = 320$, 400, 500 and 600 GeV. These figures

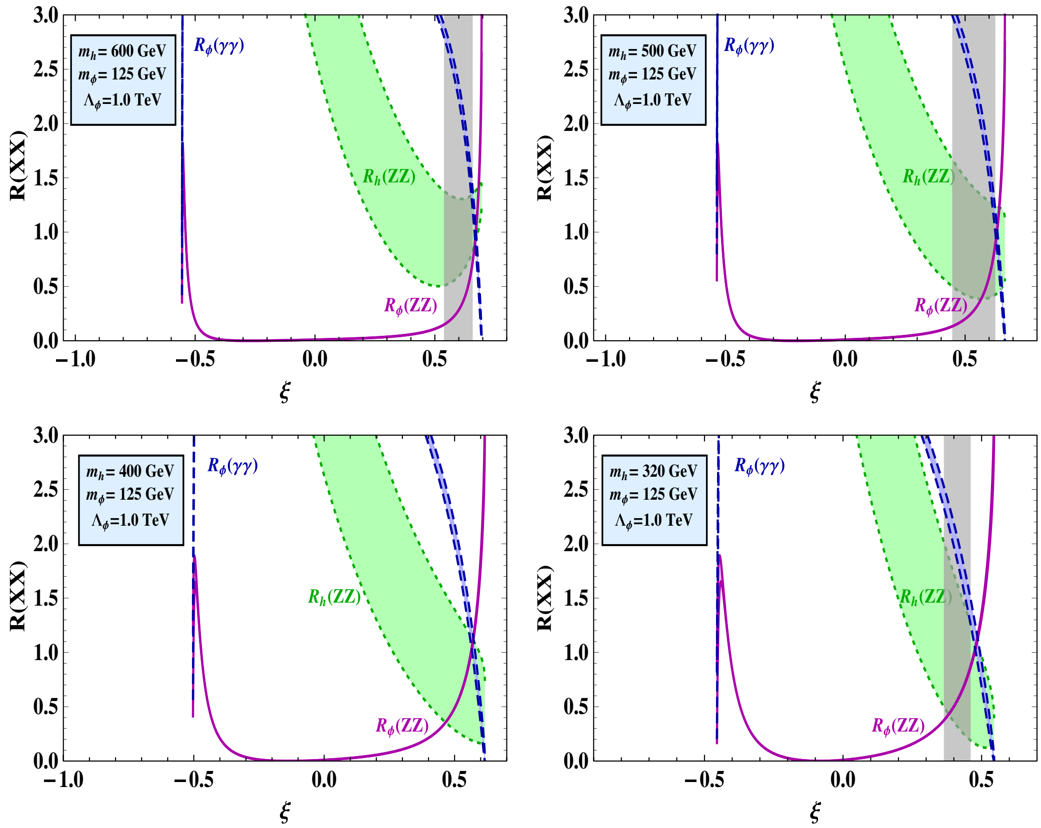

FIG. 4 (color online). Ratio of discovery significances $R(XX) \sim \sigma/\sigma_{SM}$, defined in the text, for $m_\phi = 125$ GeV, $\Lambda_\phi = 1.0$ TeV and for different masses of h. The light green bands indicate the theoretical uncertainties in the ZZ signal. There is no change in these graphs if we include the EW-corrected branching ratio to $\gamma\gamma$. We took $m_{\tau'} = 150$ GeV, precluding FCNC decays to fourth-generation leptons. The vertical gray bands indicate the allowed parameter space for ξ.

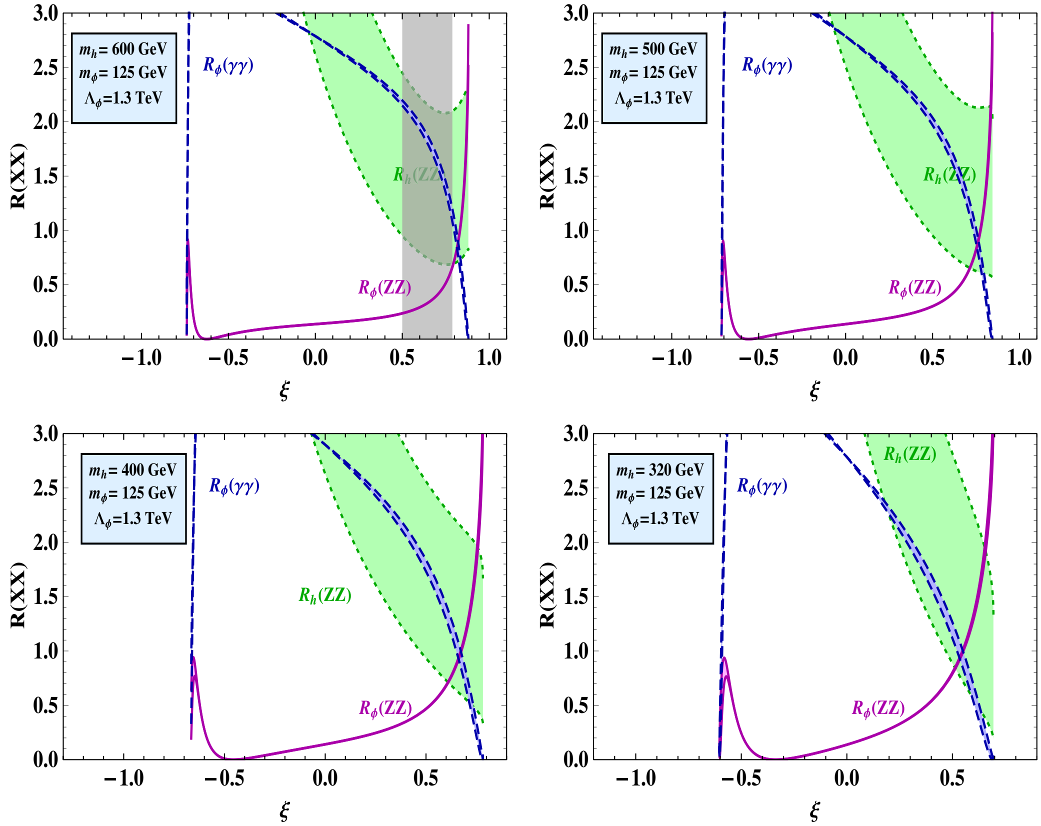

FIG. 5 (color online). Same as Fig. 4, but for $\Lambda_\phi = 1.3$ TeV.

are not affected by higher-order EW corrections to $\gamma\gamma$, as these mostly change the couplings of the heavy h field, whose couplings to $\gamma\gamma$ are irrelevant. Note that while for $\Lambda_\phi = 1$ TeV there are allowed bands for 600, 500 and 320 GeV, the parameter space for $\Lambda_\phi = 1.3$ TeV is much more restrictive and we can only fit the data for $m_h = 600$ GeV.

IV. FLAVOR-CHANGING DECAYS OF THE HIGGS-RADION STATES IN THE FOUR-GENERATION MODEL

Should the scalar discovered at the LHC be a Higgs-radion mixed state, its decay into two fermions will be different than for a SM Higgs boson, and further analysis at the LHC could differentiate the particles. In this section, we present the branching ratios of the mixed Higgs-radion state into two fermions. We start by giving analytical formulas, as they have not appeared before, then show specific values for the flavor-conserving and the flavor-violating branching ratios, for the allowed points in the parameter space presented in the previous section. The branching ratios of the mixed states ϕ and h into two fermions are given by

$$\Gamma(\phi \to \bar{f}_i f_j) = \frac{Sc}{16\pi m_\phi^3}\sqrt{m_\phi^4 + m_i^4 + m_j^4 - 2m_\phi^2 m_i^2 - 2m_\phi^2 m_j^2 - 2m_i^2 m_j^2}\,\frac{2m_i m_j}{v^2} \times ([(\tilde{c}_{ij})^2 + (\tilde{c}_{ji})^2](-m_\phi^2 + m_i^2 + m_j^2) + 4\,\mathrm{Re}[(\tilde{c}_{ij})(\tilde{c}_{ji})]m_i m_j), \quad (28)$$

$$\Gamma(h \to f_i f_j) = \frac{Sc}{16\pi m_h^3}\sqrt{m_h^4 + m_i^4 + m_j^4 - 2m_h^2 m_i^2 - 2m_h^2 m_j^2 - 2m_i^2 m_j^2}\,\frac{2m_i m_j}{v^2} \times ([(\tilde{d}_{ij})^2 + (\tilde{d}_{ji})^2](-m_h^2 + m_i^2 + m_j^2) + 4\,\mathrm{Re}[(\tilde{d}_{ij})(\tilde{d}_{ji})]m_i m_j). \quad (29)$$

Here, S is a product of statistical factors $1/j!$ for each group of j identical particles in the final state. For flavor-violating couplings, the particles in the final state are different, therefore, $S = 1$. The factor c is the color factor, for quarks $c = 3$, and for leptonic decays, $c = 1$.

TABLE II. Same as Table I, but for $m_{\tau'} = 150$ GeV.

Λ(TeV)	ξ	m(GeV)	$b'b$	tc	bs	$\tau'\tau$	$\mu\tau$	$\nu_\tau\nu_{\tau'}$
1.0	0.0283	$m_\phi = 60$	···	···	1.08×10^{-5}	···	2.83×10^{-6}	···
		$m_h = 125$	···	···	1.05×10^{-3}	···	2.88×10^{-4}	3.00×10^{-3}
1.0	0.412	$m_\phi = 125$	···	···	7.60×10^{-5}	···	2.09×10^{-5}	8.52×10^{-4}
		$m_h = 320$	···	1.61×10^{-4}	1.10×10^{-6}	9.24×10^{-3}	3.40×10^{-7}	9.76×10^{-6}
1.0	0.565	$m_\phi = 125$	···	···	5.84×10^{-5}	···	1.61×10^{-5}	7.85×10^{-4}
		$m_h = 500$	1.26×10^{-2}	6.51×10^{-5}	2.90×10^{-7}	3.62×10^{-3}	9.72×10^{-8}	2.91×10^{-6}
1.0	0.644	$m_\phi = 125$	···	···	4.50×10^{-5}	···	1.24×10^{-5}	7.28×10^{-4}
		$m_h = 600$	1.42×10^{-2}	4.76×10^{-5}	1.96×10^{-7}	2.59×10^{-3}	6.57×10^{-8}	1.99×10^{-6}

The flavor-violating couplings of the mixed states are defined as

$$\tilde{c}_{ij} = ca_{ij} + a\gamma\tilde{a}_{ij}, \qquad \tilde{d}_{ij} = da_{ij} + b\gamma\tilde{a}_{ij}, \tag{30}$$

where the couplings a_{ij} and $\tilde{a}_{ij}$, of the original unmixed Higgs and radion, have been previously obtained in [24,27] in the case of three generations and in [21,25] with four generations. In the branching ratio calculations given in the tables, we use the central values for a_{ij}'s and $\tilde{a}_{ij}$'s obtained in the numerical scans performed in the last references, and we choose a specific allowed value of ξ for each point studied in the parameter space.

We first present the branching ratios to FCNC decays for allowed parameter points from the previous section. We chose two different scenarios. In one $m_{\tau'} = 100$ GeV, thus a scalar of mass 125 GeV can have flavor-violating decays into $\tau\tau'$. These results are shown in Table I. The FCNC decay branching ratios into $\tau\tau'$ can reach 5%. Overall, the effect is not measurable, however, should the mass of the τ' be close to its experimental limit 100 GeV, the situation could change drastically and the BR($\phi \to \tau'\tau$) can reach 50%, suppressing all other decays.

In Table II, we chose $m_{\tau'} = 150$ GeV, precluding FCNC decays of the lightest scalar into fourth-generation leptons. As before, the Higgs-radion mixed state can decay into third- and fourth-generation neutrinos, but the branching ratios are not significant. For the other fourth-generation fermions, we take throughout $m_{t'} = 400$ GeV, $m_{b'} = 350$ GeV, and $m_{\nu_{\tau'}} = 90$ GeV.

We perform the same analysis, this time for the flavor-diagonal couplings, in Table III for $m_{\tau'} = 100$ GeV and in Table IV for $m_{\tau'} = 150$ GeV. As no flavor-conserving decays into fourth-generation fermions are possible, we compare the ratio of significance and Yukawa couplings to the corresponding ones in the SM. The light scalar state (at 120 or 125 GeV) exhibits large enhancements for $b\bar{b}$ and $c\bar{c}$.

The enhancements in $b\bar{b}$ for the ϕ state are consistent with the latest Tevatron results $R(b\bar{b}) = 2.03^{+0.73}_{-0.71}$ [41], while the heavier scalars have correspondingly suppressed ratios of significance with respect to the SM. The former fact is quite unlike the case for SM4, where the branching ratio BR($H \to b\bar{b}$) is 30% less than in the SM for $M_H \approx 125$ GeV [19]. The enhancements in the warped space model are inherited from the couplings of the bare Higgs boson to fermions, a_{ij}, given in [21]. The range of the flavor-conserving coefficients a_{ij} is large, and their values can accommodate the Tevatron findings (under most circumstances, they are in the same range, or only slightly reduced compared to the SM with 3 generations [27]). The final enhancements in the couplings of the physical states will give a clear indication for the warped space model.

TABLE III. Ratio of significance $R_{h(\phi)}(XX) = S(gg \to h(\phi) \to f\bar{f})S(gg \to h_{SM} \to f\bar{f})$ for different parameter space. Last column is the Yukawa couplings for $h(\phi)$ to $t\bar{t}$. The fourth-generation fermion masses are chosen as $m_{t'} = 400$ GeV, $m_{b'} = 350$ GeV, $m_{\tau'} = 100$ GeV, $m_{\nu_{\tau'}} = 90$ GeV.

Λ(TeV)	ξ	m(GeV)	R(bb)	R(cc)	R(tt)	Y_{tt}
1.5	0.0221	$m_\phi = 120$	2.05	2.13	···	0.496
		$m_h = 124$	0.563	0.557	···	0.880
1.0	0.421	$m_\phi = 125$	2.20	2.31	···	0.380
		$m_h = 320$	0.523	0.513	···	1.02
1.0	0.537	$m_\phi = 125$	1.81	1.93	···	0.317
		$m_h = 500$	0.532	0.521	0.556	1.19
1.0	0.601	$m_\phi = 125$	1.78	1.89	···	0.316
		$m_h = 600$	0.553	0.520	0.559	1.36

TABLE IV. Same as Table III, but for $m_{\tau'} = 150$ GeV.

Λ(TeV)	ξ	m(GeV)	R(bb)	R(cc)	R(tt)	Y_{tt}
1.0	0.412	$m_\phi = 125$	2.45	2.59	···	0.374
		$m_h = 320$	0.586	0.575	···	1.01
1.0	0.565	$m_\phi = 125$	2.02	2.14	···	0.334
		$m_h = 500$	0.481	0.470	0.503	1.24
1.0	0.480	$m_\phi = 125$	1.48	1.59	···	0.602
		$m_h = 600$	0.636	0.625	0.661	0.819

Because of this relative uncertanty in the fermion Yukawa couplings, we neglect higher-order EW corrections to the couplings of the Higgs with vector bosons, in the presence of a fourth generation. Moreover, these corrections have not been calculated out in the context of our scenario, in which the effects of heavy KK fermions should be included.

V. CONCLUSIONS AND OUTLOOK

In this work, we have investigated the phenomenology of the Higgs-radion mixed state with a fourth generation of quarks and leptons, in an attempt to explain the latest LHC data. We asked the question: if the scalar particle seen at the LHC is not the ordinary SM Higgs boson, but a mixed Higgs-radion state, could this state satisfy all the experimental constraints, even including the effects of a fourth generation? The four-generation assumption in warped space models is of particular interest, as the standard model with four generations, SM4, fails to reproduce the observed data to at least 95% confidence level. A fourth generation, which is severely restricted and perhaps even ruled out by the ATLAS and CMS data in SM4 could be resuscitated in warped space models. The answer to the question we posed is a cautious yes. That is, there exist regions of the parameter space where one of the mixed Higgs-radion states has mass of 125 GeV, and satisfies existing experimental constraints, while the other either has a mass of 120 GeV, thus fitting a CMS parameter point, or evades present collider bounds.

Higher-order EW corrections to the couplings of Higgs to photons in SM4 show a substantial suppression. In our scenario, however the presence of heavy KK fermions should affect such calculations and so we decided to study the predictions both with and without these corrections whose effect is to close the parameter space for the case in which the observed scalar at the LHC is the mostly Higgs state h (leaving the ϕ possibility unaffected). With no corrections to $\gamma\gamma$, if the h state is the scalar observed at the LHC, the ϕ mass must be light. Parameter points with either $m_\phi = 60$ GeV, which evade LEP restrictions, or $m_\phi = 120$ GeV, which fit the CMS data, are allowed for some range of the mixing parameter ξ. We analyzed these for both very light fourth-generation charged leptons, $m_{\tau'} = 100$ GeV, or for heavier ones, $m_{\tau'} = 150$ GeV. The difference between these two masses is that the first case allows flavor-changing decays of the Higgs-radion state, which are large in this model and which modify the branching ratios to $\gamma\gamma$ and ZZ^*. All of these parameter points require the scale Λ_ϕ to be light, in the 1.0–1.3 TeV range, the exact values dependent on the rest of the parameters. For larger m_ϕ values, the branching ratio to ZZ increases beyond the LHC limits, and thus this parameter region is forbidden. This region of parameter space is very fragile. For $m_h = 124$ GeV, the point at $m_\phi = 120$ GeV shows signs of instability as the 4ℓ excess might be cancelled by $\gamma\gamma$, while its decay into $b\bar{b}$ appears to have increased. The signal for $m_\phi = 60$ GeV, while not ruled out by LEP data depends very sensitively on the values of $m_{\tau'}$ and Λ_ϕ.

If ϕ is the scalar observed at the LHC, the h state is most likely to be heavy. The exception is when $m_{\tau'} = 100$ GeV; for $m_h = 120$ GeV parameter points exist for $\Lambda_\phi = 1.0$, 1.3, and 1.5 TeV. Regions where $m_h = 320$, 400, 500 and 600 GeV exist for some values of Λ_ϕ, which is still required to be in the 1.0–1.5 TeV range. These parameter regions seem quite robust and not dependent on whether τ' is heavy or light; however they could be ruled out within the next year at LHC as data for heavier scalars becomes available. To increase predictability of our scenario, we calculated the branching ratios of the allowed Higgs-radion states into fermions, both for flavor-changing and flavor-conserving channels (some of which are significantly enhanced with respect to the SM expectations). As more data on the scalar production and decay becomes available, these predictions can be compared with the experiment, specially noting the appearance of the interesting exotic FCNC decays.

In conclusion, we have achieved two goals in this work: first, we have shown that a scalar in a warped model with a fourth generation of fermions can be light *and* consistent with the LHC data, if the observed particle is a Higgs-radion mixed state. Second, the allowed parameter space is tightly constrained and expected to be confirmed or ruled out within a year by further analyses and/or higher luminosity at the LHC.

ACKNOWLEDGMENTS

We acknowledge NSERC of Canada for partial financial support under Grant No. SAP105354.

[1] L. Randall and R. Sundrum, Phys. Rev. Lett. **83**, 3370 (1999); **83**, 4690 (1999).

[2] K. Agashe, G. Perez, and A. Soni, Phys. Rev. D **71**, 016002 (2005); **75**, 015002 (2007); **74**, 053011 (2006); Phys. Rev. Lett. **93**, 201804 (2004); S. J. Huber and Q. Shafi, Phys. Lett. B **512**, 365 (2001); **544**, 295 (2002); **583**, 293 (2004); T. Appelquist, B. A. Dobrescu, E. Pontón, and H.-U. Yee, Phys. Rev. D **65**, 105019 (2002); T. Gherghetta, Phys. Rev. Lett. **92**, 161601 (2004); G. Moreau and J. I. Silva-Marcos, J. High Energy Phys. 01 (2006) 048; 03

(2006) 090; Eur. Phys. J. C **40**, 539 (2005); S. Chang, C. S. Kim, and M. Yamaguchi, Phys. Rev. D **73**, 033002 (2006).

[3] T. Gherghetta and A. Pomarol, Nucl. Phys. **B586**, 141 (2000); Y. Grossman and M. Neubert, Phys. Lett. B **474**, 361 (2000).

[4] H. Davoudiasl, J. L. Hewett, and T. G. Rizzo, Phys. Lett. B **473**, 43 (2000); A. Pomarol, Phys. Lett. B **486**, 153 (2000); S. Chang, J. Hisano, H. Nakano, N. Okada, and M. Yamaguchi, Phys. Rev. D **62**, 084025 (2000).

[5] K. Agashe, A. Delgado, M. J. May, and R. Sundrum, J. High Energy Phys. 08 (2003) 050; K. Agashe and R. Contino, Nucl. Phys. **B742**, 59 (2006); K. Agashe, R. Contino, L. Da Rold, and A. Pomarol, Phys. Lett. B **641**, 62 (2006); M. Carena, E. Ponton, J. Santiago, and C. E. M. Wagner, Nucl. Phys. **B759**, 202 (2006); Phys. Rev. D **76**, 035006 (2007); R. Contino, L. Da Rold, and A. Pomarol, Phys. Rev. D **75**, 055014 (2007); A. D. Medina, N. R. Shah, and C. E. M. Wagner, Phys. Rev. D **76**, 095010 (2007); C. Bouchart and G. Moreau, Nucl. Phys. **B810**, 66 (2009).

[6] S. J. Huber and Q. Shafi, Phys. Lett. B **498**, 256 (2001); C. Csaki, A. Falkowski, and A. Weiler, J. High Energy Phys. 09 (2008) 008; M. Blanke, A. J. Buras, B. Duling, S. Gori, and A. Weiler, J. High Energy Phys. 03 (2009) 001.

[7] W. D. Goldberger and M. B. Wise, Phys. Rev. Lett. **83**, 4922 (1999).

[8] C. Csaki, J. Hubisz, and S. J. Lee, Phys. Rev. D **76**, 125015 (2007).

[9] G. F. Giudice, R. Rattazzi, and J. D. Wells, Nucl. Phys. **B595**, 250 (2001).

[10] C. Csáki, M. L. Graesser, and G. D. Kribs, Phys. Rev. D **63**, 065002 (2001).

[11] G. Aad *et al.* (ATLAS Collaboration), Phys. Lett. B **710**, 49 (2012).

[12] S. Chatrchyan *et al.* (CMS Collaboration), Phys. Lett. B **710**, 26 (2012).

[13] J. A. Casas, J. R. Espinosa, and M. Quiros, Phys. Lett. B **382**, 374 (1996).

[14] G. Burdman and L. Da Rold, J. High Energy Phys. 12 (2007) 086; G. Burdman, L. Da Rold, and R. D'E. Matheus, Phys. Rev. D **82**, 055015 (2010).

[15] B. Holdom, Phys. Rev. D **54**, R721 (1996); M. Maltoni, V. A. Novikov, L. B. Okun, A. N. Rozanov, and M. I. Vysotsky, Phys. Lett. B **476**, 107 (2000); H. J. F. He, N. Polonsky, and S. f. Su, Phys. Rev. D **64**, 053004 (2001); V. A. Novikov, L. B. Okun, A. N. Rozanov, and M. I. Vysotsky, Phys. Lett. B **529**, 111 (2002); G. D. Kribs, T. Plehn, M. Spannowsky, and T. M. P. Tait, Phys. Rev. D **76**, 075016 (2007); P. Bechtle, O. Brein, S. Heinemeyer, G. Weiglein, and K. E. Williams, Comput. Phys. Commun. **182**, 2605 (2011); O. Eberhardt, A. Lenz, and J. Rohrwild, Phys. Rev. D **82**, 095006 (2010); D. Fargion, M. Yu. Khlopov, R. V. Konoplich, and R. Mignani, Phys. Rev. D **54**, 4684 (1996).

[16] S. A. Cetin, G. W. S. Hou, V. E. Ozcan, A. N. Rozanov, and S. Sultansoy, arXiv:1112.2907.

[17] G. Aad *et al.* (ATLAS Collaboration), arXiv:1202.3389; (ATLAS Collaboration), arXiv:1202.3076; (ATLAS Collaboration), arXiv:1202.5520; (ATLAS Collaboration), arXiv:1202.6540.

[18] CMS Collaboration, Report No. CMS PAS HIG-12-008 [http://cdsweb.cern.ch/record/1429928/files/HIG-12-008-pas.pdf].

[19] E. Kuflik, Y. Nir, and T. Volansky, arXiv:1204.1975v1; O. Eberhardt, G. Herbert, H. Lacker, A. Lenz, A. Menzel, U. Nierste, and M. Wiebusch, arXiv:1204.3872; A. Djouadi and A. Lenz, arXiv:1204.1252.

[20] T. Aaltonen *et al.* (CDF and D0 Collaboration), Phys. Rev. D **82**, 011102 (2010).

[21] M. Frank, B. Korutlu, and M. Toharia, Phys. Rev. D **84**, 075009 (2011).

[22] S. Bae, P. Ko, H. S. Lee, and J. Lee, Phys. Lett. B **487**, 299 (2000); K. M. Cheung, Phys. Rev. D **63**, 056007 (2001); J. L. Hewett and T. G. Rizzo, J. High Energy Phys. 08 (2003) 028; D. Dominici, B. Grzadkowski, J. F. Gunion, and M. Toharia, Acta Phys. Pol. B **33**, 2507 (2002); M. Toharia, Phys. Rev. D **79**, 015009 (2009); K. Huitu, S. Khalil, A. Moursy, S. K. Rai, and A. Sabanci, Phys. Rev. D **85**, 016005 (2012).

[23] D. Dominici, B. Grzadkowski, J. F. Gunion, and M. Toharia, Nucl. Phys. **B671**, 243 (2003).

[24] A. Azatov, M. Toharia, and L. Zhu, Phys. Rev. D **80**, 031701 (2009).

[25] M. Frank, B. Korutlu, and M. Toharia, Phys. Rev. D **84**, 115020 (2011).

[26] K. Agashe and R. Contino, Phys. Rev. D **80**, 075016 (2009).

[27] A. Azatov, M. Toharia, and L. Zhu, Phys. Rev. D **80**, 035016 (2009).

[28] H. de Sandes and R. Rosenfeld, Phys. Rev. D **85**, 053003 (2012); V. Barger, M. Ishida, and W.-Y. Keung, Phys. Rev. D **85**, 015024 (2012); Phys. Rev. Lett. **108**, 101802 (2012); K. Cheung and T.-C. Yuan, Phys. Rev. Lett. **108**, 141602 (2012); B. Grzadkowski, J. F. Gunion, and M. Toharia, Phys. Lett. B **712**, 70 (2012).

[29] S. Chatrchyan *et al.* (CMS Collaboration), arXiv:1203.5410v1.

[30] G. Aad *et al.* (ATLAS Collaboration), arXiv:1202.3076v1.

[31] G. Aad *et al.* (ATLAS Collaboration), J. High Energy Phys. 04 (2012) 069.

[32] C. Charmousis, R. Gregory, and V. A. Rubakov, Phys. Rev. D **62**, 067505 (2000).

[33] J. F. Gunion, M. Toharia, and J. D. Wells, Phys. Lett. B **585**, 295 (2004).

[34] G. Passarino, C. Sturm, and S. Uccirati, Phys. Lett. B **706**, 195 (2011).

[35] S. Actis, G. Passarino, C. Sturm, and S. Uccirati, Nucl. Phys. **B811**, 182 (2009).

[36] S. Actis, G. Passarino, C. Sturm, and S. Uccirati, Nucl. Phys. **B670**, 12 (2008).

[37] A. Denner, S. Dittmaier, A. Muck, G. Passarino, M. Spira, C. Sturm, S. Uccirati, and M. M. Weber, arXiv:1111.6395.

[38] A. Azatov, M. Toharia, and L. Zhu, Phys. Rev. D **82**, 056004 (2010).

[39] J. F. Gunion, H. E. Haber, G. L. Kane, and S. Dawson, Front. Phys. **80**, 1 (2000).

[40] S. Casagrande, F. Goertz, U. Haisch, M. Neubert, and T. Pfoh, J. High Energy Phys. 09 (2010) 014.

[41] TEVNPH (Tevatron New Phenomena and Higgs Working Group), CDF, and D0 Collaborations, arXiv:1203.3774; W. Fisher (CDF and D0), in "Proceedings of Moriond 2012," (unpublished) [http://indico.in2p3.fr/getFile.py/].